Analysis of Surface Blistering in the Manufacturing of Faucets

Picha Panmongkol[1] and Noppakorn Phuraya[2*]

[1]Department of Mechanical Engineering, Faculty of Engineering, Thonburi University, Bangkok, 10160, Thailand

[2]Department of Industrial Engineering, Faculty of Engineering, Mahidol University, Nakornprathom, 73170, Thailand

*** Corresponding author, Email address: Noppakorn.phu@mahidol.edu**

Abstract

This research aimed to carry out an analysis of the surface blistering problem involved in the manufacturing process for faucets. Zamak 3 is a raw material produced by using a high-pressure die-casting process. The surface blistering microstructure was examined with an optical microscope and scanning electron microscope, while gas properties were examined by using the gas chromatography technique. The results from optical and scanning electron microscopy showed that discontinuities occur in the zinc layer, including a large amount of porosity spreading all over the product on the surface of the zinc layer as well as blistering under the surface. The gas chromatography results showed that the average amount of hydrogen gas was 0.00755 percent per gram, assuming that the discontinuities are caused by the porosity containing gas inside the base metal surface and the heat that occurs during the process of liquid metal injection is the main factor driving gas expansion which affects the discontinuities.

Keywords: Surface blistering, Faucet, Zamak 3, High pressure Die-casting (HPDC), Gas chromatography

1. Introduction

Zamak 3 is the most common Zamak alloy and a popular material for die-casting (Kaye & Street, 2016). Zamak comprises a family of alloys with zinc as the base metal and aluminum, magnesium, and copper as alloy elements. Zamak is widely used in the production of automotive parts, furniture accessories, appliance components, faucets and taps, shower hinges, handles, valves and pneumatics, toys, ornaments, clothing, and mechanical parts, as well as in other industries and applications (Campbell, 2015; Wang, Turnley, & Savage, 2011; Schweitzer, 2003). Different Zamak alloys are suitable for different uses. When it comes to Zamak 3 alloy, it is usually considered the first choice for zinc die-casting (Zhao, Wang, Li, & Xia, 2009). The high pressure die-casting process uses high pressure to inject molten metal into the mold cavity until it is filled by casting in a hot chamber (Zhao, Wang, & Xia, 2009). Commonly used with alloys that have a low melting point, such as zinc alloy, it has a melting temperature range of approximately 420 degrees Celsius. The outstanding feature of the hot furnace metal casting machine is that the temperature of the molten metal maintained during injection, which shortens the casting time and increases productivity (Campbell, 2015).

Surface blistering is a form of defect that occurs in the high-pressure die-casting process. It is caused by the entrainment of gases within each sub-surface layer of the metal when metal is injected into the mold (Armillotta, Fasoli, & Guarinoni, 2016). Panossian et al. (Panossian & Ferrari, 2004) studied blistering problems in zinc-plated steel and zinc-plated die-cast zinc alloy parts. The results revealed that blistering was caused by a variety of factors. For zinc-plated steel parts, it was caused by inadequate pre-treatment, and for zinc-plated die-cast zinc alloy parts, it was caused by poor substrate surface quality.

Oksana et al. (Ozhoga-Maslovskaja, Gariboldi, & Lemke, 2016) studied the conditions for blister formation during thermal cycles of Al-Si-Cu-Fe alloys for high pressure die-casting. The results found that blisters developed from pores below a critical aspect ratio, as a result of high plastic strain accumulation in localized regions lying between the pore and outer surface (ligament).

Reveko et al. (Reveko & Moller, 2018) studied the special aspects of electrodeposition on zinc die casting, which showed that zinc and aluminum are well-known chemically active elements, especially in the molten state. These metals can react with moisture and other substances present in the mold, leading to gas formation. As a reaction product, hydrogen can be easily dissolved in the molten metal. Subsequently, molecular hydrogen together with some trapped air forms bubbles when the melt starts to solidify, which remain in the bulk since the outer solid skin is already formed, resulting in inner porosity.

In this study, an analysis of surface blistering on the faucet resulting from high-pressure die-casting was conducted to determine its root cause. The surface blistering and the nearby microstructure were observed and analyzed using optical microscopy (OM) and scanning electron microscopy (SEM). Gas chromatography was employed to inspect the entrainment of gases within the sub-surface layer of the metal. The interpretation of the study's results facilitated the provision of recommendations for mitigating surface blistering defects in future manufacturing processes.

2. Material and Methods

In this research, Zamak 3 was utilized as the material for the faucets. The chemical composition of the faucets was analyzed using an optical emission spectrometer (OES) (Hitachi, model OE750). The specific chemical composition of the faucets is presented in

Table 1. Chemical composition of faucet

Element	Zn	Al	Cu	Fe	Mg	Si
Weight (%)	94.49	4.72	0.574	0.0628	0.0436	0.011

Three samples (B1, B2, and B3) of the metallographic samples exhibiting surface blistering were sectioned using a cut-off wheel. The metallographic specimens were then polished with silicon carbide paper and diamond paste, followed by etching with a solution of 5 ml nitric acid in 100 mL of ethanol. The swab technique was applied for 5 seconds during etching. Post-etching, the samples were thoroughly washed with flowing water and alcohol, and then dried using hot air.

The metallographic examination was conducted using optical microscopy (OM) with a Nikon model: Eclipse Nvdia-N light microscope. Microscopic tests were complemented by chemical microanalysis using the energy dispersive spectrometry (EDS) method and scanning electron microscopy (SEM) to characterize the presence of precipitate phases. The SEM tests were performed with a JEOL model: JSM-6610LV.

The gas analysis was conducted using gas chromatography with the GC 7890A machine equipped with a thermal conductivity detector (TCD). The procedure involved: 1) Selecting four samples from the faucet body with blistering issues for testing; 2) Preparing test pieces by cutting them into small sizes suitable for vials, placing them into four tubes

(including one tube without a test piece for comparison); 3) Weighing each workpiece in the vials and recording the values for calculations, followed by placing the vials in an oven at 80 degrees Celsius for 30 minutes; 4) Extracting the gas inside the vial using a syringe; 5) Calculating the proportion of hydrogen gas per weight to facilitate a comparison of gas amounts in each vial using Equation (1), as illustrated in Figure 1 (a-d).

$$Hydrogen\ per\ weight\ ratio = \frac{Hydrogen\ (percent)}{weight\ (gram)} \quad (1)$$

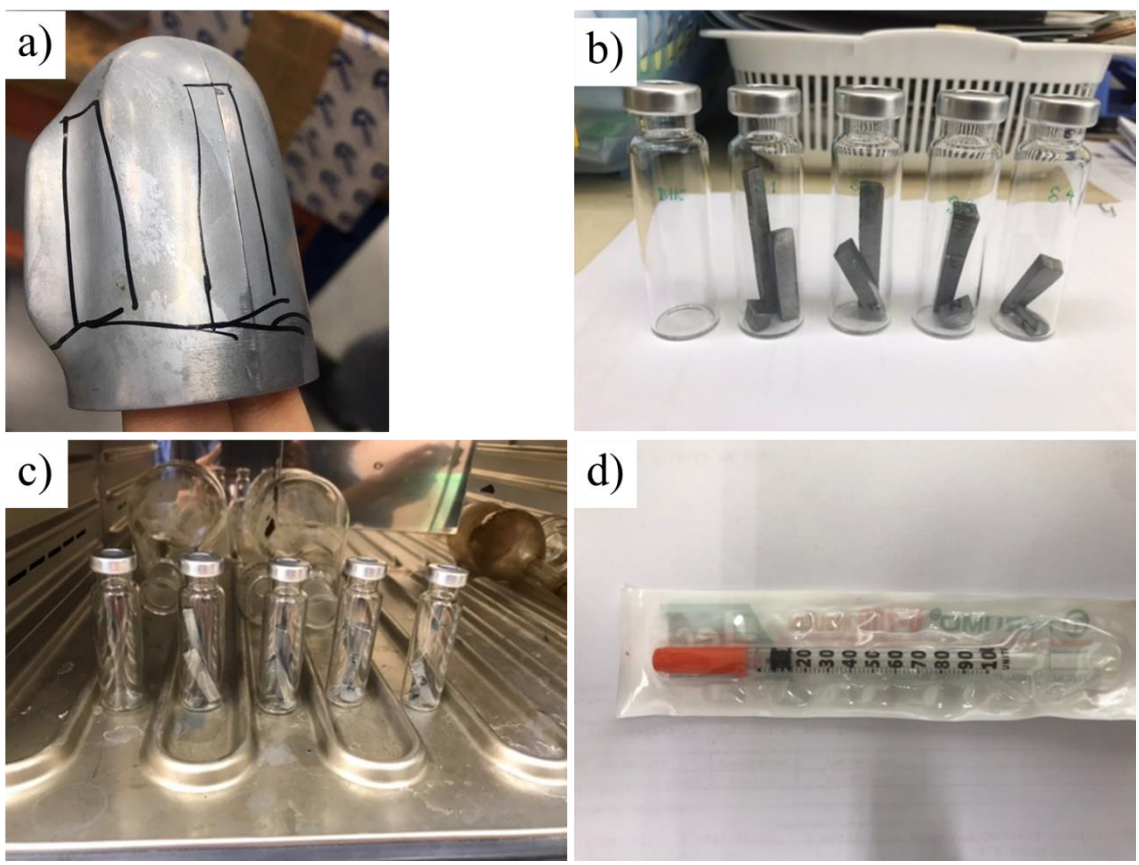

Figure 1. Gas Chromatography set-up

3 RESULTS AND DISCUSSION

3.1 Visual examination

The results of the macroscopic observations performed on specimens B1, B2, and B3 found surface blistering with a size of around 1 mm, which was found after electroplating and polishing to make the surface shiny and have the desired properties. The coating process has 3 layers of coating: copper, nickel, and chromium, respectively. The surface blistering is shown in Figure 2.

Surface blistering in zinc die-casting typically occurs due to the entrapment of gases, often nitrogen or hydrogen, within the molten zinc during the die-casting process. These gases can get trapped as the metal solidifies, resulting in the formation of surface blisters (Sakuragi, Fuwa, Nakayama, & Nagamori, 2020; (Pola, Tocci, & Goodwin, 2020).

In the case of surface blistering on a faucet, the process involves compressing the air within a high-pressure die-cast machine and ejecting the component from the mold using mechanisms such as a vacuum valve, overflow system, or vent. Any residual air present inside the casting dissolves uniformly into the molten metal. The air turbulence within the process can lead to localized air concentration, resulting in high-pressure cavities. After the electroplating process, the faucet also undergoes heating, causing any accumulated air beneath the applied coating to escape. This release of trapped air can lead to the formation of blisters on the faucet surface. (Dybowski, Kiełbus, & Poloczek, 2023)

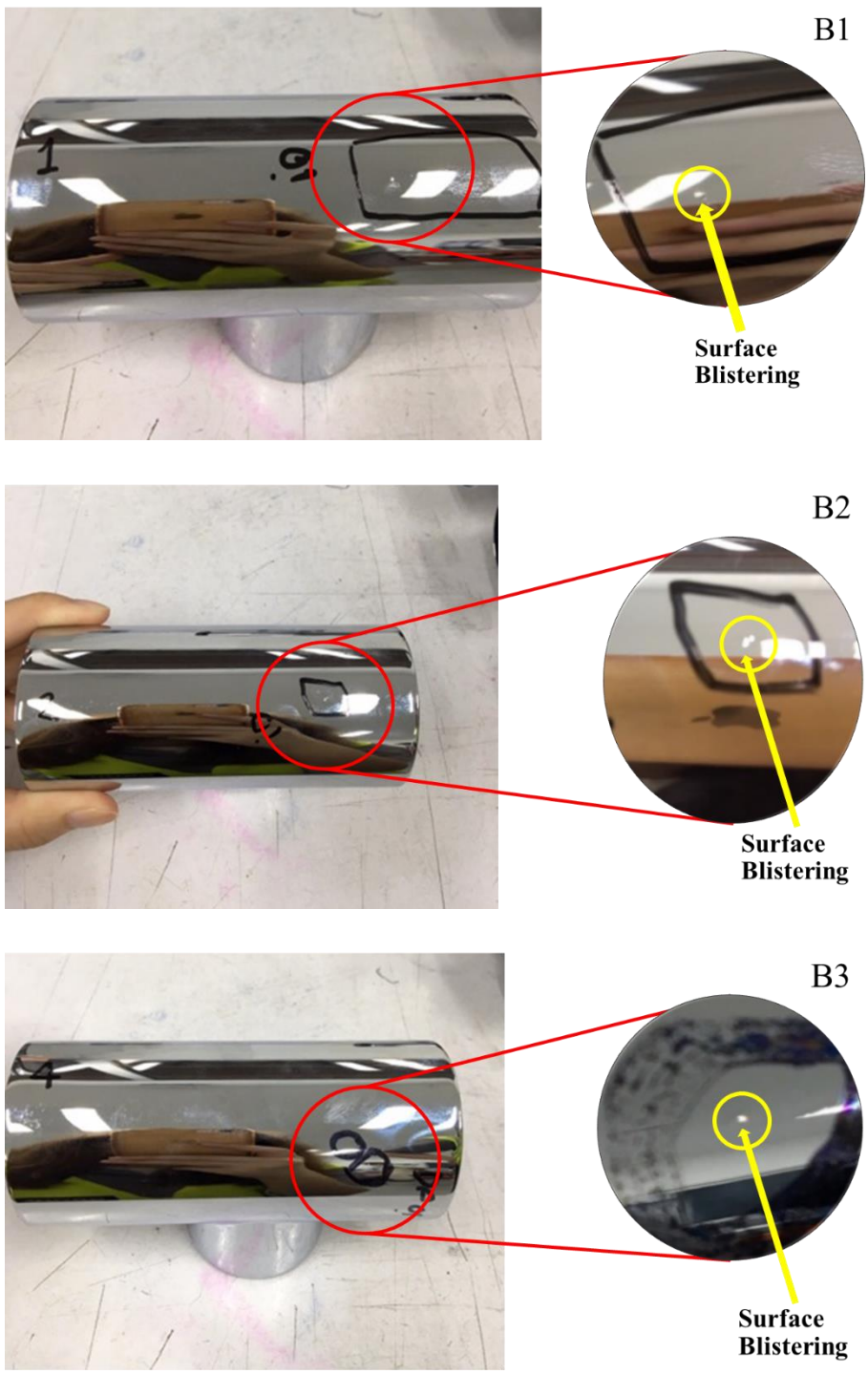

Figure 2. Results of visual examination showing the surface blistering on specimens B1, B2, and B3

3.2 Structural characterization by optical microscopy and scanning electron microscopy

The typical microstructure of specimens in Figures 3 (a, c, and e) illustrates that the chill zone of a workpiece features fine grains. Deeper within the material, dendritic grains are evident in the columnar zone. As we progress towards the center of the workpiece, known as the equiaxed zone, the grains maintain a rounded shape similar to those near the surface, though they are larger in size. (Ares, & Schvezov, 2007; Zhang, Shortle et al., 2019; Ares, & Gassa, 2012)

Figures 3 (b, d, and f) revealed a coating consisting of two layers. The first layer is copper, with thicknesses of 21.72, 19.27, and 23.00 micrometers, respectively. On top of this layer lies another layer composed of nickel and chromium, measuring 6.42, 5.27, and 5.65 micrometers in thickness, respectively. Additionally, there is a discontinuity layer, situated beneath the copper layer, and also found copper inserts into the discontinuity area and cracks at the Ni and Cr layers. This crack arises from localized plastic strains occurring at different temperatures during the electroplating process. (Ozhoga-Maslovskaja, Gariboldi, & Lemke, 2016).

Figure 4 illustrates the detailed microstructures of the as-annealed sample, characterized by back-scattering electrons (BSE). As depicted in Figure 4 (a), the microstructure reveals the presence of η-Zn, while Figure 4 (b) highlights the eutectic phase consisting of fine Zn and Al phases (Hasan, Sharif, & Gafur, 2020; (Liang, Wu, Sandlöbes, Korte-Kerzel, & Schmid-Fetzer, 2019). The Zn matrix is observed to contain fine α-Al phases are depressively. Al particles with varying sizes form under different conditions; specifically,

the eutectic-phase Al particles crystallize at high temperatures, while ultrafine-grained Al particles precipitate in the Zn matrix during cooling, attributed to decreased solubility (Pola, Tocci, & Goodwin, 2020).

Figure 5 displays the SEM-EDS results of the base material (specimen B1). Upon closer examination, several distinct phases were identified through point analysis. The Spectrum 1 area exhibits the η-Zn-rich, characterized by round, white regions distributed along the grain boundaries. Spectrum 2, analyzed over an area, displays a eutectic structure consisting of two phases intermixed between the η-Zn phase and the α-Al phase. Quantitative elemental analysis techniques were employed to determine the composition of these phases: 1) The η-Zn phase (Pola, Tocci, & Goodwin, 2020) is identified as a phase with a substantial amount of zinc dissolved in the form of a solid solution, constituting a zinc-rich solid solution. This phase has a higher quantity of zinc than what is proportionally expected based on the total weight of zinc in the workpiece. 2) Conversely, the α-Al phase contains a relatively high concentration of aluminum dissolved in the form of a solid solution mixed with zinc. (Pola, Tocci, & Goodwin, 2020) It was also observed that the amount of aluminum element in this phase was higher than what would be expected proportionally based on the total weight of the aluminum element in the workpiece. (Pola, Tocci, & Goodwin, 2020)

The presence of carbon suggests an active role in contamination within the microstructure. The quantitative measurement of carbon in the Energy Dispersive X-ray Spectroscopy (EDS) analysis may be attributed to the die lubricant agents on the mold surface. It has been reported that the formation of the reaction occurs during the die-casting process. For example, if the lubricant agent is octadecane, the reaction would be $C_{18}H_{38} = 18C + 19H_2$.

This reaction illustrates the generation of carbon and molecular hydrogen. Carbon remains effective as a barrier for the melt, and hydrogen additionally contributes to the development of internal porosity. (Reveko & Moller, 2018)

The microstructures of specimens B1, B2, and B3 were examined using scanning electron microscopy, and the results are presented in Figure 6. In all three specimens, discontinuities were identified beneath the coating surface. Figures 6 (a), (c), and (e) are images obtained through backscattered electron imaging (BEI), which enhances the contrast between elements with different atomic numbers, allowing for a clear visualization of the grain characteristics in each structure. On the other hand, Figures 6 (b), (d), and (f) display secondary electron images (SEI). These images provide depth-of-field information, enabling the identification of areas where discontinuities, such as hollow regions, are present, making it possible to analyze the elemental composition of both the bulging surface and the discontinuities within the blistering surface.

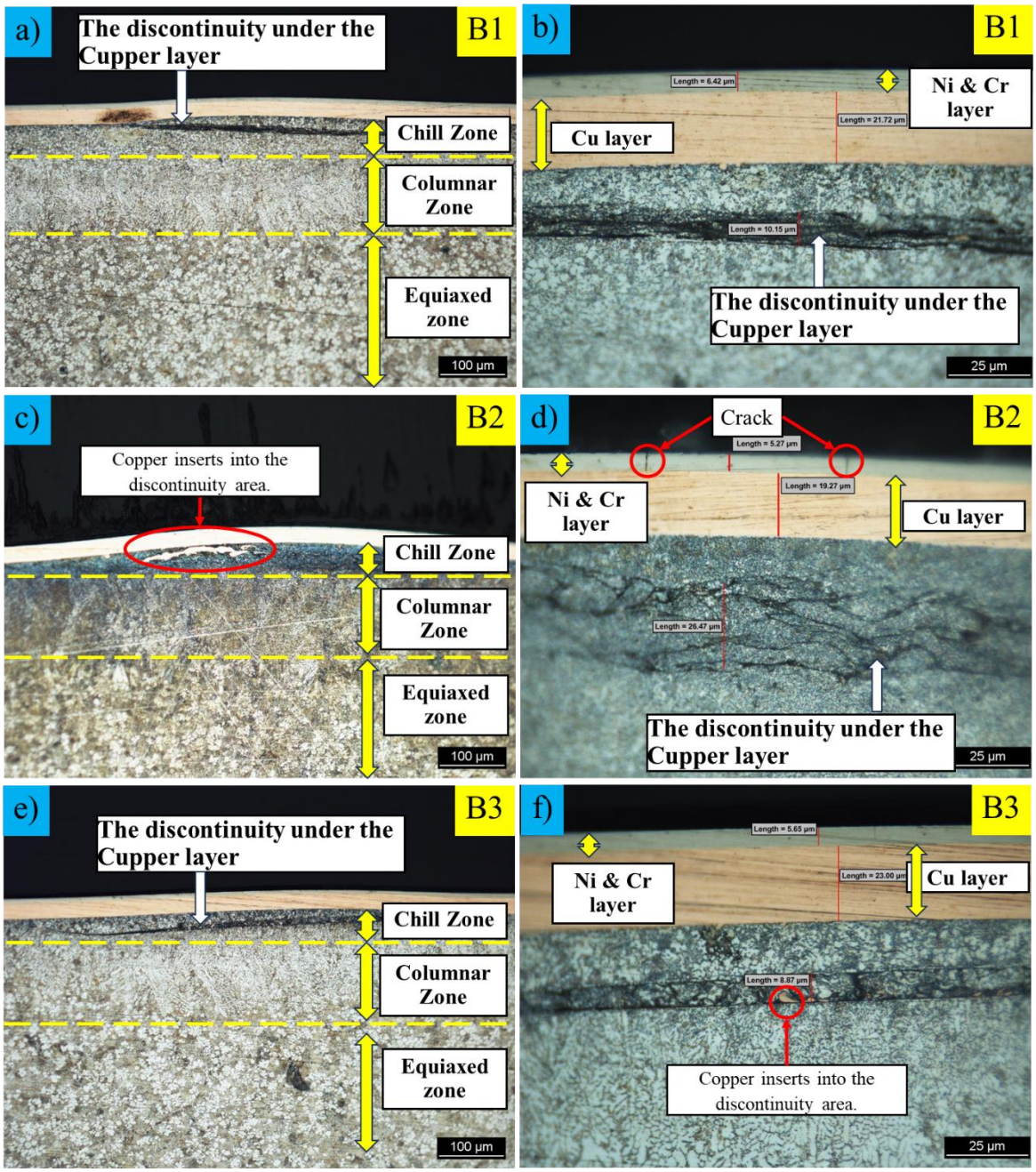

Figure 3. The cross-sections of blistered specimen B1, B2, and B3.

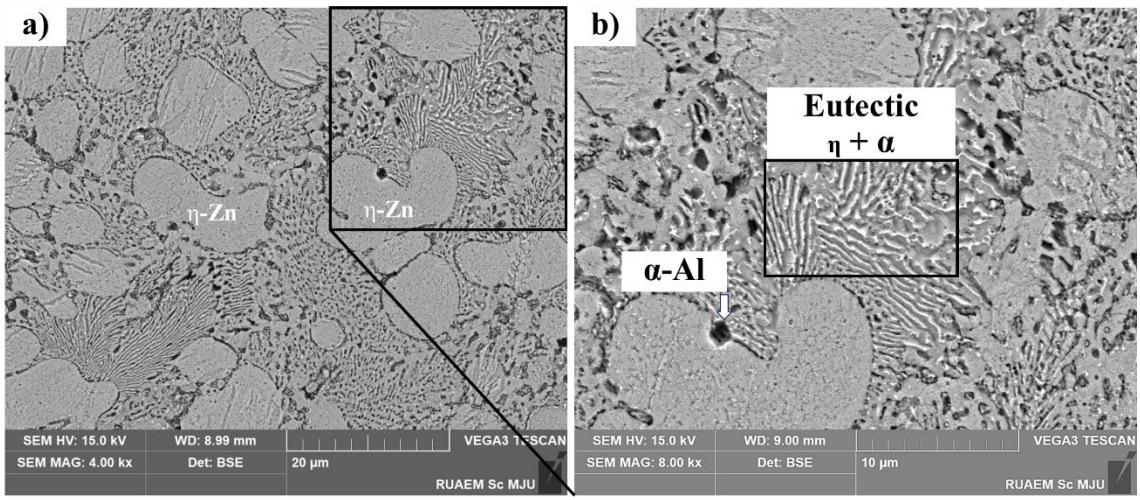

Figure 4 Typical morphology of the base material (specimen B1): (a) η-Zn phase (b) α-Al particles and the eutectic lamellar morphology (η+ α).

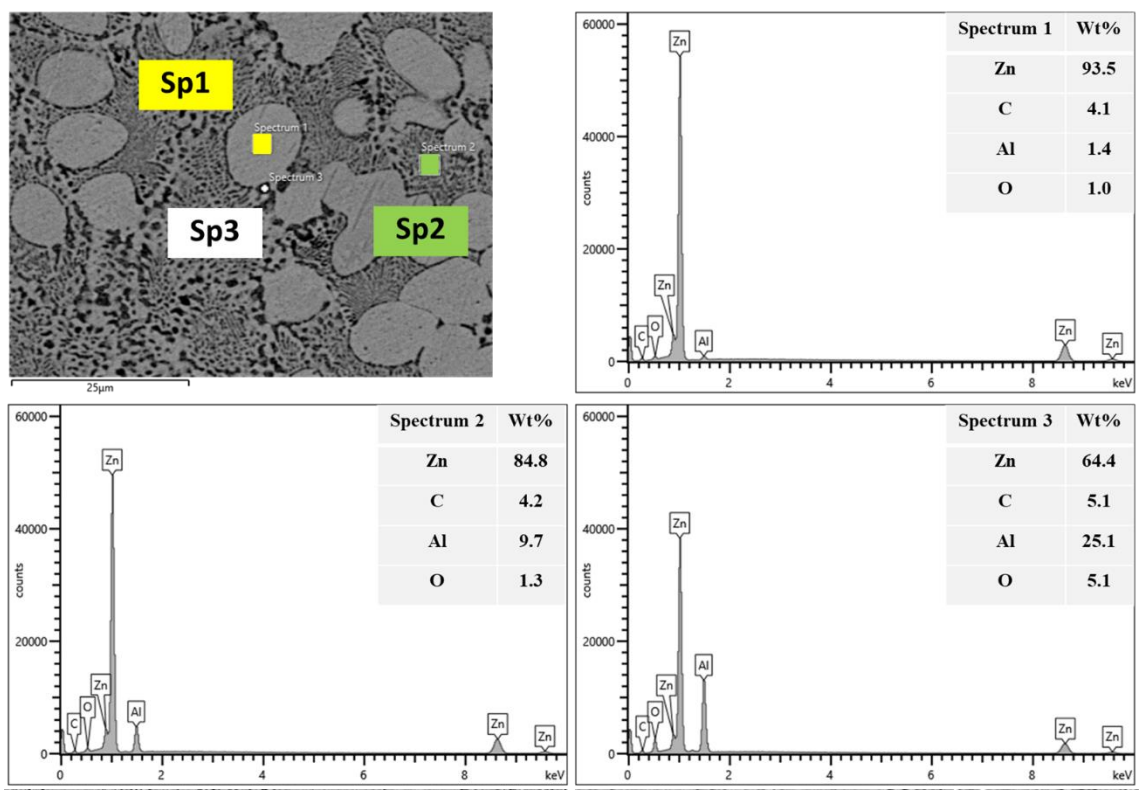

Figure 5. SEM-EDS results for the base material (specimen B1).

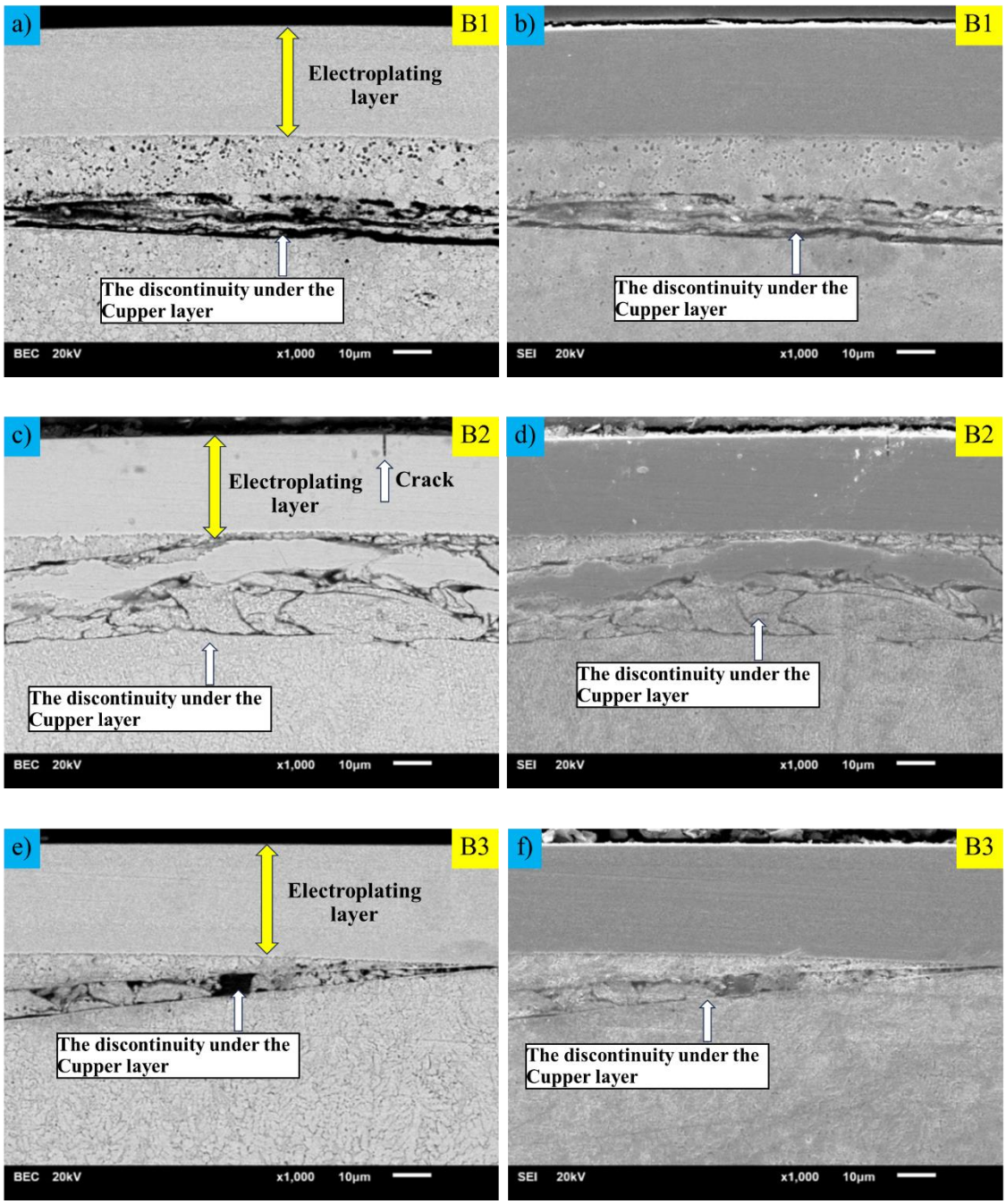

Figure 6. SEM (BEC and SEI) results of the specimen B1, B2, and B3.

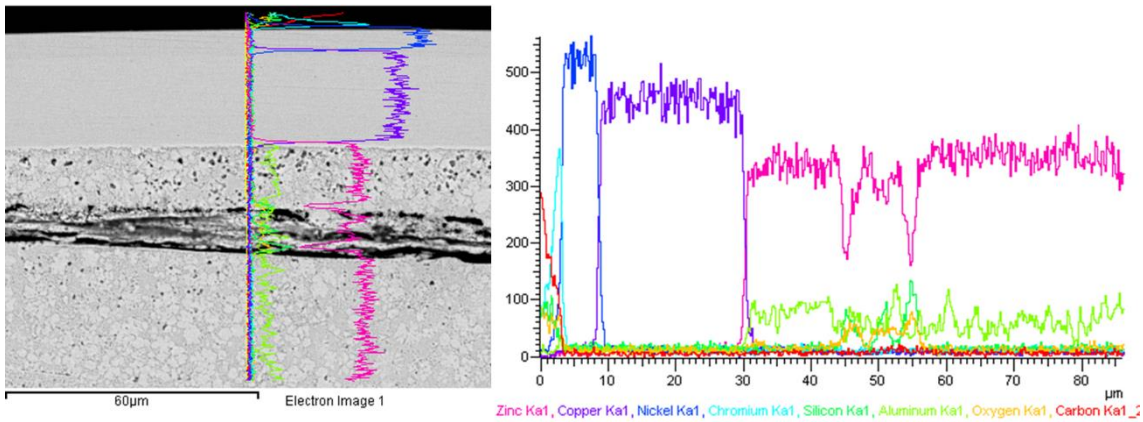

Figure 7. Graph showing the number of elements in the surface blistering area

Figure 7 reveals the elemental content of the workpiece by applying a line scanning technique to the surface blistering, which found that the amount of zinc decreased suddenly in the area of the blistering surface, which indicated that the material had disappeared in that area and a gap had formed. Elemental analysis using linear scanning techniques also confirmed that the coating had three layers comprised of chromium, nickel, and copper, with each layer having a thickness of approximately 3 micrometers, 6 micrometers, and 21 micrometers, respectively.

3.3 Results of gas inspection using gas chromatography techniques

The gas inspection results for each sample were obtained using gas chromatography techniques, and the findings are presented in Table 2**.**

Table 2 displays the hydrogen gas concentrations found in four specimens**.** Specimen 1 exhibited a hydrogen gas concentration of 0**.**1537 percent, while Specimen 2 had a hydrogen gas concentration of 0**.**1213 percent, Specimen 3 had a hydrogen gas concentration of 0**.**1313

percent, and the fourth specimen contained 0.1282 percent hydrogen gas. Since the specimens varied in size and weight, it was necessary to calculate the proportion of hydrogen gas to weight for comparison. Specimen 1 had a hydrogen gas concentration of 0.0083 percent per gram, while Specimen 2 had 0.0072 percent per gram of hydrogen gas, Specimen 3 had 0.0071 percent per gram of hydrogen gas, and Specimen 4 had 0.0076 percent per gram of hydrogen gas.

Table 2. Amount of hydrogen gas found in the workpieces using gas chromatography techniques

Compound Name	**Results (%Norm)**			
	Sample 1	**Sample 2**	**Sample 3**	**Sample 4**
Sample Weight (grams)	18.5709	16.9007	18.6004	16.7804
Hydrogen	0.1537	0.1213	0.1313	0.1282
%Hydrogen per weight (%/g)	0.0083	0.0072	0.0071	0.0076
Everage %Hydrogen per weight (%/g)	0.00755			

In zinc die casting, blistering can occur due to various factors including the electroplating process. Blistering involves the formation of bubbles or blisters on the surface of the zinc die-cast part after electroplating. It is often considered a defect that can impact the appearance and functionality of the final product. For specimens B1, B2, and B3, surface blistering was detected after the electroplating process.

The electroplating process can contribute to blistering in zinc die-casting (Panossian & Ferrari, 2004; Reveko & Moller, 2018) due to contamination, in which contaminants on

the surface of the zinc die-cast part, such as oils, greases, or residual mold release agents, can create a barrier between the metal surface and the electroplating solution. This barrier can trap gases released during the electroplating process, leading to the formation of blisters. Hydrogen evolution can also contribute to blistering. During electroplating, hydrogen gas is produced at the cathode (the zinc die-cast part being plated). If the electroplating process is not properly controlled, excessive hydrogen evolution can occur. Hydrogen gas can become trapped in pores, imperfections, or microstructures on the surface of the die-cast part, leading to the formation of blisters as the gas accumulates. Inadequate cleaning can likewise impact blistering. Proper cleaning and the preparation of the zinc die-cast part before electroplating are crucial to removing any contaminants and ensuring good adhesion of the electroplated layer. Inadequate cleaning can leave behind impurities that contribute to blistering. Finally, porosity in the die-cast can affect blistering. Zinc die-casting processes can sometimes result in parts with porosity, which are tiny voids or pores within the material. If these pores are not properly sealed or filled before electroplating, they can act as sites for gas entrapment, leading to blistering.

4. Conclusions

The microstructure layers of specimens B1, B2, and B3 can be categorized into three regions: chill region, columnar region, and equiaxed region. The thickness of each region depends on the cooling rate of the specimen. Additionally, the thickness of the chill area is influenced by the duration of polishing of the workpiece before plating. During examination using Backscattered Electron Imagery (BEI) and Secondary Electron Imagery (SEI), it was

observed that voids formed at the discontinuity mark beneath the area where the surface blistering and pores were distributed throughout the workpiece. The microstructure consists of two types of structures and phases: the η phase, characterized by a round white appearance, and the eutectic structure, which is a mixture of two phases, namely the η phase and α phase, appearing as scattered white and black stripes. A layer of discontinuity is present in the zinc layer, located beneath the blistering surface. This suggests that the blistering surface results from the high-pressure casting process are caused by trapped gas within the discontinuity layer being stimulated by external factors such as heat, leading the trapped gas to push the material outwards. Gas chromatography techniques were used to examine the gas content in the workpieces, revealing the presence of hydrogen gas with an average concentration calculated at 0.00755 percent/weight in each workpiece sample. Controlling gas production in casting workpieces, particularly in high-pressure casting processes, is typically challenging.

Acknowledgments

This research project is supported by Mahidol University.

References

Ares, A. E., & Gassa, L. M. (2012). Corrosion susceptibility of Zn–Al alloys with different grains and dendritic microstructures in NaCl solutions. *Corrosion Science*, *59*, 290-306. Retrieved from https://doi.org/10.1016/j.corsci.2012.03.015

Ares, A. E., & Schvezov, C. E. (2007). Influence of solidification thermal parameters on the columnar- to- equiaxed transition of aluminum- zinc and zinc- aluminum

alloys. *Metallurgical and Materials transactions A*, *38*, 1485-1499. Retrieved from https://doi-org.ejournal.mahidol.ac.th/10.1007/s11661-007-9111-z

Armillotta, A., Fasoli, S., & Guarinoni, A. (2016). Cold flow defects in zinc die casting: prevention criteria using simulation and experimental investigations. *The International Journal of Advanced Manufacturing Technology*, *85*, 605- 622. Retrieved from https://doi.org/10.1007/s00170-015-7959-4

Campbell, J. (2015). *Complete casting handbook: metal casting processes, metallurgy, techniques and design*. Butterworth-Heinemann.

Diehl, D., Schneider, E. L., & Clarke, T. G. R. (2021). Formation of hydrogen blisters during the solution treatment for aluminum alloys. *Tecnologia em Metalurgia, Materiais e Mineração*, *18*, 0-0. Retrieved from https://doi.org/10.4322/2176-1523.20212374

Dybowski, B., Kiełbus, A., & Poloczek, Ł. (2023). Effects of die-casting defects on the blister formation in high- pressure die- casting aluminum structural components. *Engineering Failure Analysis*, 107223. Retrieved from https://doi.org/10.1016/j.engfailanal.2023.107223

Hasan, M. M., Sharif, A., & Gafur, M. A. (2020). Characteristics of eutectic and near-eutectic Zn–Al alloys as high-temperature lead-free solders. *Journal of Materials Science: Materials in Electronics*, *31*, 1691- 1702. Retrieved from https: / / doi-org.ejournal.mahidol.ac.th/10.1007/s10854-019-02687-x

Kaye, A., & Street, A. (2016). *Die casting metallurgy: Butterworths monographs in materials*. Elsevier.

Liang, S. M., Wu, Z., Sandlöbes, S., Korte-Kerzel, S., & Schmid-Fetzer, R. (2019). Analysis of microstructure formation in cast Zn alloys derived from computational thermodynamics of the Zn– Al– Cu– Mg system. *Journal of Materials Science*, *54*(13), 9887-9906. Retrieved from https://10.1007/s10853-019-03553-1

Ozhoga-Maslovskaja, O., Gariboldi, E., & Lemke, J. N. (2016). Conditions for blister formation during thermal cycles of Al–Si–Cu–Fe alloys for high pressure die-casting. *Materials & Design*, *92*, 151- 159. Retrieved from https://doi.org/10.1016/j.matdes.2015.12.003

Panossian, Z., & Ferrari, J. V. (2004). Case studies of blistering problems in zinc-plated steel and zinc-plated die-cast zinc alloy parts. *Plating and surface finishing*, *91*(9), 48-52.

Pola, A., Tocci, M., & Goodwin, F. E. (2020). Review of microstructures and properties of zinc alloys. *Metals*, *10*(2), 253. Retrieved from https://doi:10.3390/met10020253

Reveko, V., & Moller, P. (2018). Special aspects of electrodeposition on zinc die castings. *Nasf Surface Technology White*, *82*(8), 1-9.

Sakuragi, T., Fuwa, D., Nakayama, I., & Nagamori, T. (2020). Reduction of Blister Occurrence after Plating in Zinc Alloy Die Casting by Optimization of Gating System. *Materials Transactions*, *61*(12), 2393-2401. Retrieved from https://doi.org/10.2320/matertrans.MT-M2020222

Schweitzer, P. A. (2003). *Metallic materials: physical, mechanical, and corrosion properties* (Vol. 19). CRC press.

Wang, L., Turnley, P., & Savage, G. (2011). Gas content in high pressure die castings. *Journal of Materials Processing Technology*, *211*(9), 1510-1515. Retrieved from https://doi.org/10.1016/j.jmatprotec.2011.03.024

Zhang, W., Du, Y., Huo, W., Hu, J., Lu, J., Zhao, X., ... & Zhang, Y. (2019). Microstructure and Mechanical Properties of Zamak 3 Alloy Subjected to Sliding Friction Treatment. *Metallurgical and Materials Transactions A*, *50*, 5888-5895. Retrieved from https://doi.org/10.1007/s11661-019-05466-9

Zhao, H. D., Wang, F., Li, Y. Y., & Xia, W. (2009). Experimental and numerical analysis of gas entrapment defects in plate ADC12 die castings. *Journal of materials processing technology*, *209*(9), 4537-4542. Retrieved from https://doi.org/10.1016/j.jmatprotec.2008.10.028

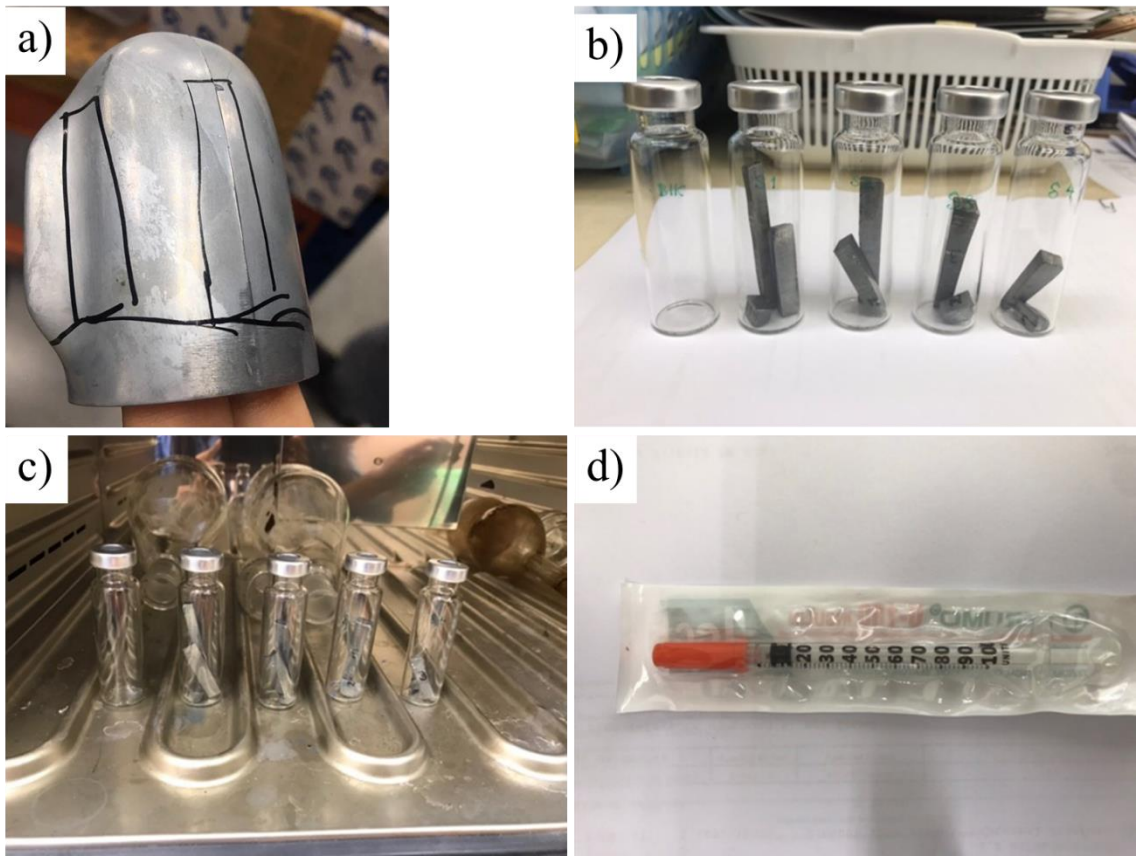

Figure 1. Gas Chromatography set-up

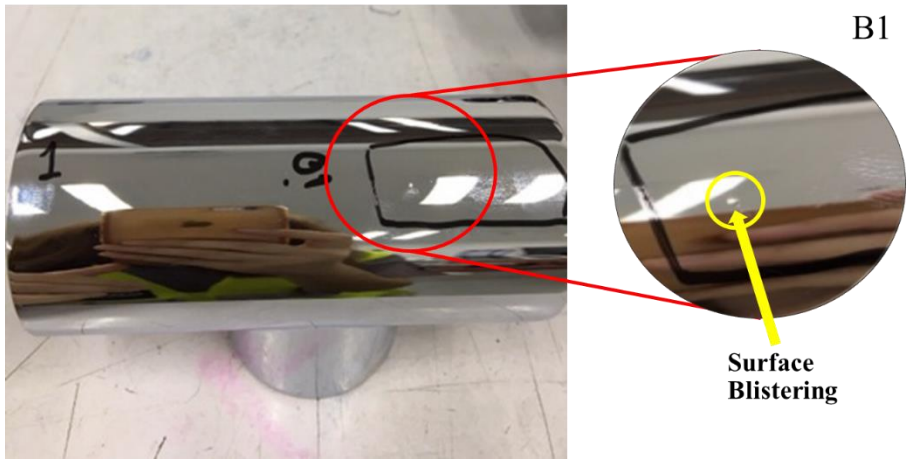

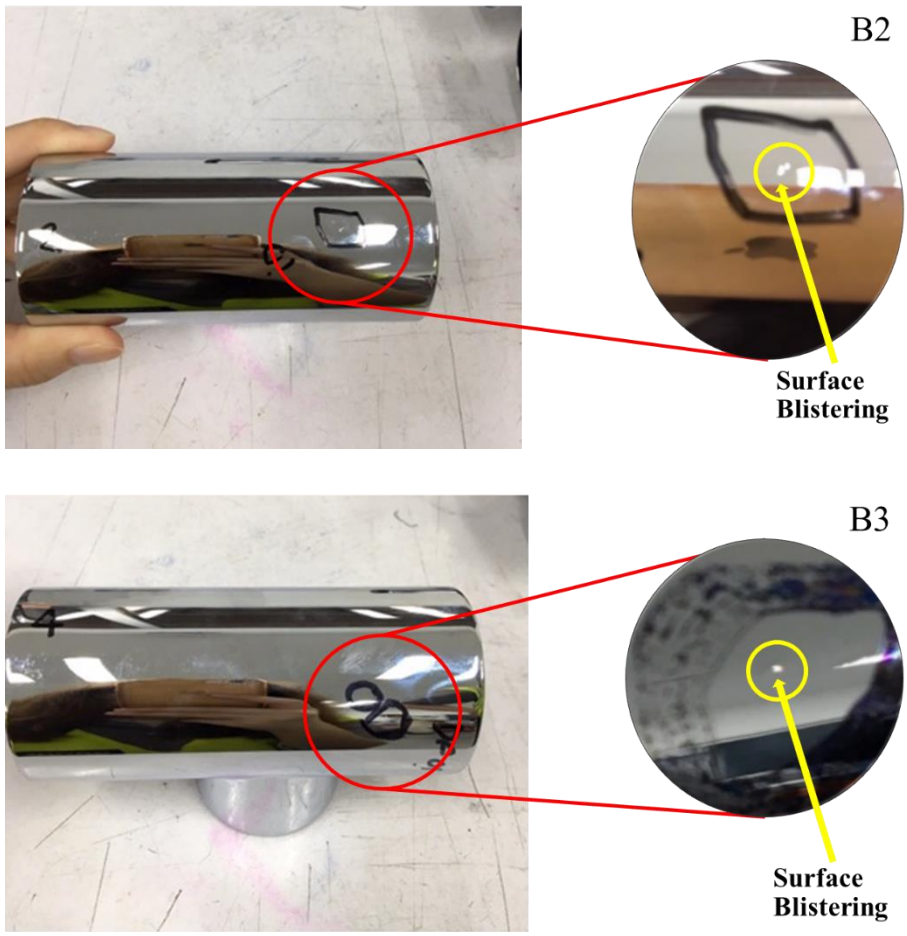

Figure 2. Results of visual examination showing the surface blistering on specimens B1, B2, and B3

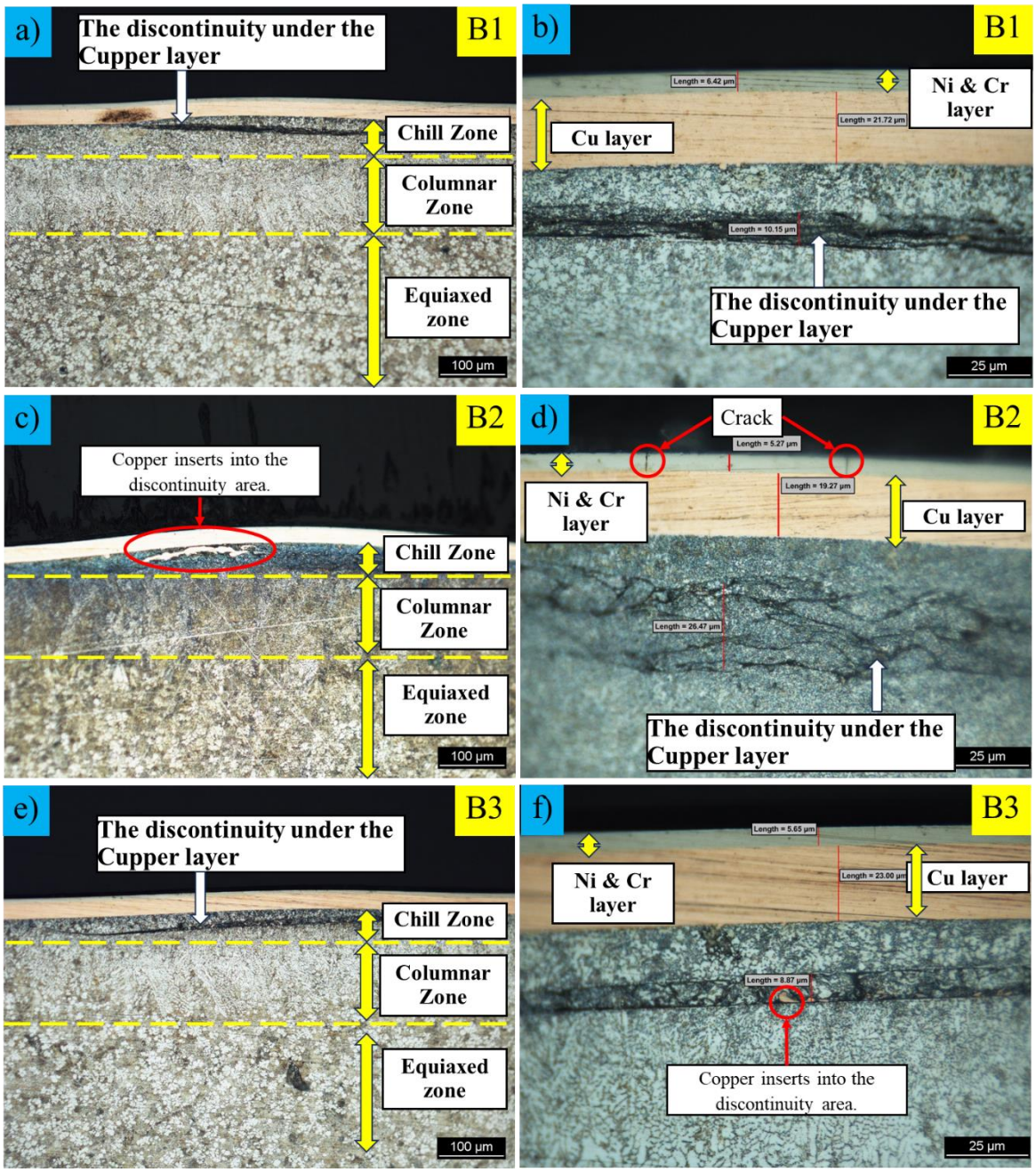

Figure 3. The cross-sections of blistered specimen B1, B2, and B3.

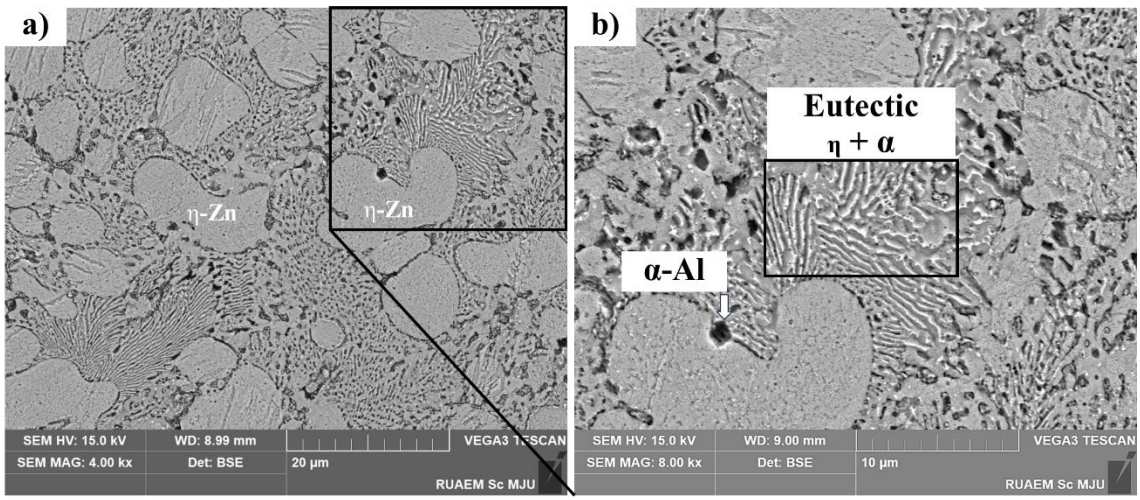

Figure 4 Typical morphology of the base material (specimen B1): (a) η-Zn phase (b) α-Al particles and the eutectic lamellar morphology (η+ α).

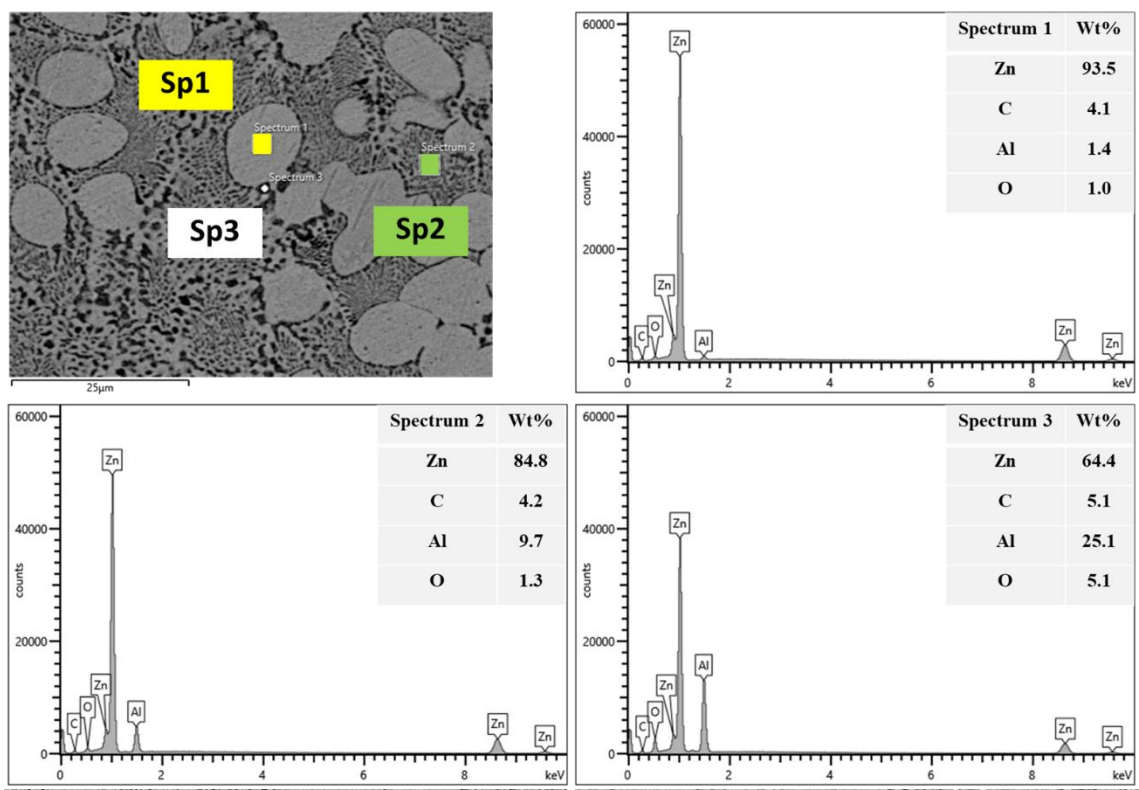

Figure 5. SEM-EDS results for the base material (specimen B1).

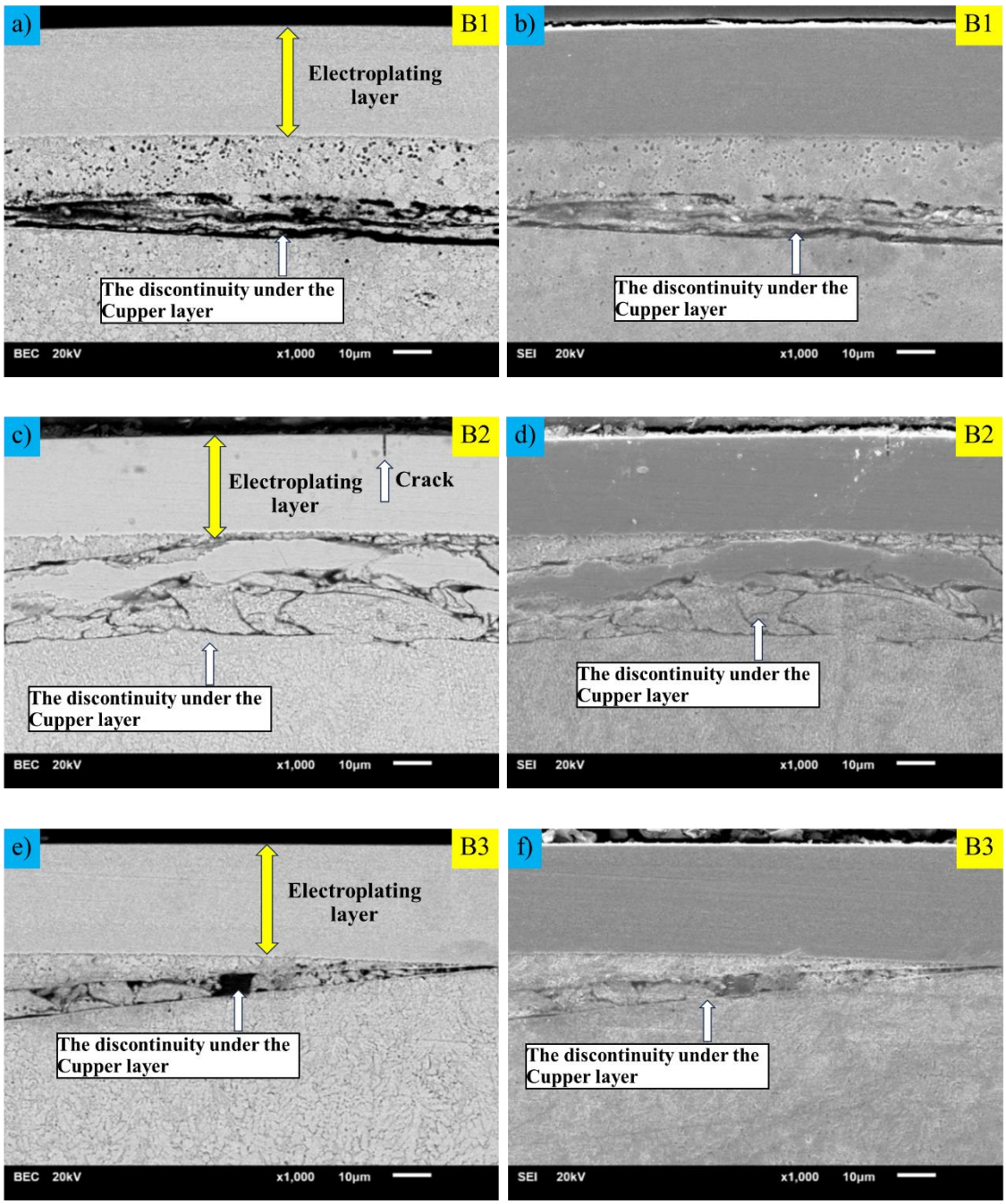

Figure 6. SEM (BEC and SEI) results of the specimen B1, B2, and B3.

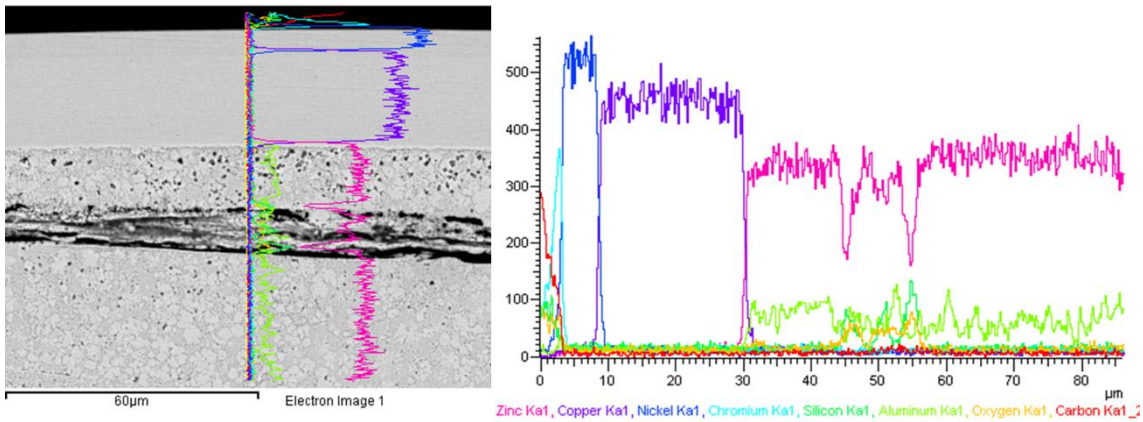

Figure 7. Graph showing the number of elements in the surface blistering area

Table 1. Chemical composition of faucet

Element	Zn	Al	Cu	Fe	Mg	Si
Weight (%)	94.49	4.72	0.574	0.0628	0.0436	0.011

Table 2. Amount of hydrogen gas found in the workpieces using gas chromatography techniques

Compound Name	Results (%Norm)			
	Sample 1	Sample 2	Sample 3	Sample 4
Sample Weight (grams)	18.5709	16.9007	18.6004	16.7804
Hydrogen	0.1537	0.1213	0.1313	0.1282
%Hydrogen per weight (%/g)	0.0083	0.0072	0.0071	0.0076
Everage %Hydrogen per weight (%/g)	0.00755			